EASR

Engineering and Applied Science Research

https://www.tci-thaijo.org/index.php/easr/index

Published by the Faculty of Engineering, Khon Kaen University, Thailand

Scheffe's models for optimization of tensile and flexural strength of recycled ceramic tile aggregate concrete

Edidiong E. Ambrose[1)], Fidelis O. Okafor[2)] and Michael E. Onyia*[2)]

[1)]Department of Civil Engineering, Faculty of Engineering, Akwa Ibom State University, Ikot Akpaden, Akwa Ibom State, Nigeria
[2)]Department of Civil Engineering, Faculty of Engineering, University of Nigeria, Nsukka, Nigeria

Received 25 October 2020
Revised 27 January 2021
Accepted 1 February 2021

Abstract

The large amount of wastes generated by the ceramic industry is presently not reused in any significant quantity. Incorporation of these wastes into concrete production is a win-win proposition for both the ceramic and concrete industries. However, there are presently no mathematical models for predicting the properties of these concretes. While there has been extensive research on the use of ceramic wastes as coarse aggregates, there are very limited research data on their use as fine aggregates. In the current study, augmented Scheffe's simplex lattice theory was used to formulate mathematical models for predicting and optimizing the tensile and flexural strengths of concrete into which recycled ceramic tiles (RCT) are incorporated as a fine aggregate. Preliminary tests on RCT show that it is a suitable fine aggregate material and further testing shows the feasibility of using it in concrete production. It has also been established that addition of RCT improves the strength of concrete. The formulated models can predict the mix ratio for desired tensile and flexural strengths of RCT concrete and vice versa. Responses from these models are in agreement with corresponding experimental data. Adequacy of the models was confirmed using analysis of variance and normal probability plots of model residuals at a 95% confidence level. With the model equations, tensile and flexural strength of potential mix proportions of RCT concrete can be monitored and optimized. This is especially important for concrete used in pavement, airfield slabs and water retaining structures, among other applications.

Keywords: Concrete, Flexural strength, Modelling, Recycled ceramic waste, Scheffe's theory, Tensile strength

1. Introduction

Concrete has become the most commonly used construction material [1]. Its demand is ever increasing because of its versatility and sustainability [2]. Over 33 billion tonnes of concrete are produced annually [3]. However, this is not without huge environmental impacts. Concrete consumption has led to a rapid depletion in the natural reserves of conventional materials used as aggregates in its production [4]. Given the need for sustainable development in our built environment, incorporation of industrial wastes and by-products into concrete has been established as yielding immense benefits [5-7]. These benefits include reuse and recycling, reduction of environmental pollution, economic benefits and improved durability of concrete. Recently, ceramic wastes have attracted the attention of numerous researchers. There has been growing interest in its use as an aggregate material in concrete production [8-11]. Ceramic wastes are waste products from the manufacture of earthen wares, porcelain, ceramic tiles, electrical insulators, sanitary ware and bricks, among others. Some of these wastes are generated during manufacture as a result of production errors, glazing faults, cracks, off-standard products and size discrepancies [6]. Other losses occur during transportation and distribution to end users. However, the greatest percentage of ceramic waste is from construction and demolition wastes [12]. Ceramics are non-biodegradable [9, 13]. Thousands of tonnes of these wastes are generated annually all over the world. Currently, they are disposed of in landfills [9, 14] with no significant recycling [9, 14, 15]. Thus, incorporating these wastes into concrete production could be a win-win proposition. Doing so could aid in solving the environmental problems associated with ceramic wastes in landfills and also lead to more sustainable concrete production.

Most research on incorporation of ceramic wastes into concrete production are on its use as aggregates [9-18], mainly as coarse aggregates. However, the few available data on its use as fine aggregates are encouraging. Awoyera et al. [14] studied concrete manufactured with recycled ceramic tile as a fine aggregate. They observed that its split tensile strength was better than that of concrete made with conventional aggregates. The difference was directly proportional to the percentage of replacement of conventional aggregate with ceramic waste. This was found even with high performance concrete (HPC). Bartosz et al. [18] reported that the split tensile strength of HPC with 100% recycled ceramic aggregate was 34.25% higher than that of the same material with conventional aggregate. Similar results have been reported by other authors [10, 13].

Tensile and flexural strength are very important properties of concrete, although compressive strength is usually considered the more important. Tensile strength of a concrete section determines its resistance to cracking. According to Paewchompoo et al. [19], the initial corrosion-induced cracking time of concrete is determined by the tensile strength and modulus of elasticity of the section.

*Corresponding author. Tel.: +23 480 3382 1550
Email address: michael.onyia@unn.edu.ng
doi: 10.14456/easr.2021.52

Hence, this is an important parameter in the design of highways and airfield slabs [20] as well as in design of water retaining structures, where crack control is critical. Unreinforced concretes rely on their flexural strength to resist bending. This is typical in unreinforced concrete road pavement and runways, which rely on their flexural strength to distribute vehicular loads over a wider area [21]. Mix designs for pavement are mostly based on flexural strength data. It is therefore of great importance to estimate the strength properties of potential mix proportions of concrete. However, there are presently no models providing such estimations for concrete incorporating ceramic waste aggregates. Thus, this study aims to formulate mathematical models for predicting and optimizing tensile as well as flexural strength of concrete with partial or full replacement of river sand with recycled ceramic tile (RCT) as a fine aggregate.

1.1 Modelling of concrete strength properties

Concrete strength is an engineering measure of the ability of concrete members to resist loads. It is of great importance in structural applications. Thus, predicting the strength properties of concrete has long attracted the attention of researchers, although most efforts have focused on compressive strength. In formulating mathematical models for predicting concrete strength, the use of analytical methods [22-24], artificial neural networks [25-27] and empirical methods [28-31] are common. However, the most appealing technique is the empirical approach, which makes use of regression equations. The general form of multiple linear regression equations used to model concrete strength is given by Equation 1.

$$Y = a_0 + a_1X_1 + a_2X_2 + a_3X_3 + ... + a_mX_m \quad (1)$$

where $a_0 - a_n$ are regression coefficients and $X_1 - X_n$ are independent variables that determine concrete strength. This approach has been used by many researchers to model concrete strength using several concrete parameters [31]. The deficiency of Equation 1 is that the variables are assumed to be linearly related, which does not reflect the true situation with concrete strength. These parameters are not always linearly related and they are often interrelated. To overcome this deficiency, a number of non-linear models have been adopted. They include logarithmic transformed non-linear correlations [32, 33] and higher degree polynomial regressions. Quadratic regression is the most commonly used of the polynomial models, usually taking the form of Equation 2.

$$Y = a_0 + \sum_{i=1}^{m} a_iX_i + \sum_{i=j=1}^{m} a_{ij}X_iX_j \quad (2)$$

In this study, we aim to derive quadratic polynomial regression models for predicting the characteristic tensile and flexural strengths of concrete using Scheffe's lattice simplex theory. The models employ proportions of concrete mix components that are transformed into pseudo-components of the simplex factor space. The innovative aspect of the models is the incorporation of both sand and RCT as fine aggregates in the mix.

1.2 Scheffe's simplex lattice theory

Appropriate design substantially reduces the number of experiments, especially in multi-component systems. Simplex lattice design is an experimental design methodology for modelling response and component relationships. A lattice is an ordered distribution of points in a regular pattern, while a simplex lattice is a structural representation of lines or planes joining assumed coordinates or points representing components of a mixture [34-37]. Simplex lattice designs are simply referred to as Scheffe's simplex lattice design [37]. According to Scheffe's theory, if q denotes the number of mixture components, $X_1, X_2, X_3, ... X_q$, in a mixture design and the degree of polynomial to be fitted to the design is denoted by n, then each component of the mixture resides on a vertex of a simplex lattice in a (q-*1*) factor space such that a $\{q, n\}$ simplex lattice consists of uniformly spaced points defined by all the possible combinations of (n+*1*) levels of each component [38, 39]. When q = 2, a straight line represents the lattice simplex. For q = 3, the simplex lattice is an equilateral triangle, while for q =4, it is a regular tetrahedron with each vertex representing each of the components.

Simplex lattice design is only applicable in experiments of mixtures in which the response depends on the mass or volume proportions of individual components and not on their total mass or volume [34, 36, 39, 40]. Properties of concrete depend on an adequate mass or volume proportioning of its constituents and not on its total mass or volume. Thus, Scheffe's optimization theory can be used to model and optimize concrete properties. Scheffe introduced polynomial regressions to model responses. The general form of the polynomial equation of degree n in a q-component mixture (usually referred to as $\{q, n\}$ polynomials) is given as Equations 3 and 4.

In linear form (n = 1): $\hat{y} = \sum_{1 \le i \le q} \beta_iX_i \quad (3)$

In quadratic form (n = 2): $\hat{y} = \sum_{1 \le i \le q} \beta_iX_i + \sum_{1 \le i \le j \le q} \beta_{ij}X_iX_j \quad (4)$

where $\hat{y}$ is the mixture property (response), β values are the polynomial coefficients and X values are the mixture component ratios by weight or volume. Properties of a $\{q, n\}$ simplex lattice design for a multi-variable function, $F(X_1, X_2, X_3, ... X_q)$ are defined when:

a) The sum of the component proportions are unity and no component has a negative value. Mathematically these can be represented as:

$$X_1 + X_2 + ... + X_q = \sum_{i=1}^{q} X_i = 1 \quad (5)$$

$$0 \le X_i \le 1 \quad (6)$$

b) The number of terms in a polynomial equation, which is also the minimum number of design points required to determine coefficients of the resulting model, is given as:

$$N = C_n^{q+n-1} = \frac{(q+n-1)!}{(q-1)!(n)!} \quad (7)$$

c) Coefficients of the polynomial equations can be expressed as functions of expected responses (y_i) at the design and control points of the simplex. The general relationship between the two is given as Equation 8.

$$\beta_i = y_i \; and \; \beta_{ij} = 4y_{ij} - 2y_i - 2y_j \quad (8)$$

1.2.1 Interaction of components in Scheffe's factor space

Mixture components in Scheffe's simplex design are evenly distributed in the factor space of the simplex and the proportions assumed by each component are *n+1* equally spaced levels from 0 to 1 based on Equation 9. Thus, for a second-degree polynomial simplex design (n = 2), each component must take the levels: 0, ½ and 1 while for a cubic polynomial (n = 3), the levels are: 0, ⅓, ⅔ and 1.

$$X_i = 0, \frac{1}{n}, \frac{2}{n}, \ldots 1 \quad (9)$$

Consider a {*4, 2*} simplex lattice, as in Figure 1, of which the factor space is a tetrahedron. Each component assumes proportions of 0, ½, and 1 based on Equation 9. There are ten design points at the boundaries. The vertices of the tetrahedron correspond to the number of terms in Scheffe's second-degree polynomial in Equation 4 based on Equation 7. The four vertices of the simplex are defined by (1,0,0,0); (0,1,0,0); (0,0,1,0) and (0,0,0,1), representing single component mixtures, while the remaining six points each at the middle of each of the edges represent binary blends of two component mixtures.

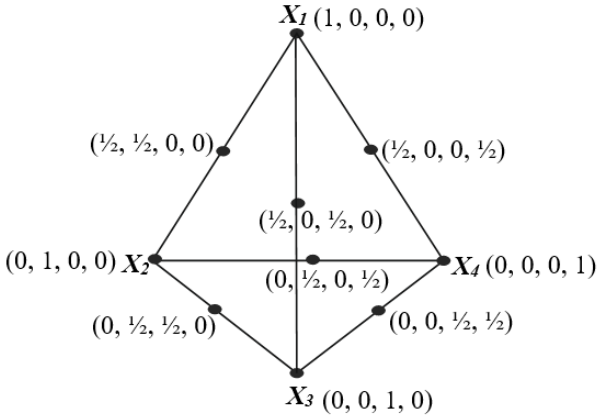

Figure 1 A {4, 2} Scheffe's simplex lattice showing pseudo-ratios at design points

1.3 Augmented simplex centroid design

Simplex lattice design is a saturated design [39, 41] containing just the necessary design points needed to formulate the model equations. These design points are only at the vertices and edges of the simplex. Thus, the design does not give any information about the inside of the simplex. It is sometimes necessary to augment and improve simplex design by incorporating additional points within the simplex. These additional points, referred to as check points, are used in testing the adequacy of a fitted model. Generally, augmented centroid design is achieved by introducing additional design points at the centroid and midway between the centroid and each of the vertices [4]. Augmented simplex centroid design still maintains the model equation form of a simplex lattice design. However, estimated model coefficients differ slightly from those obtained using only simplex lattice design points. These coefficients improve the accuracy of model prediction.

2. Materials and methods

2.1 Materials

Five materials were used in laboratory experiments during this study. Cement and water served as a binder, while river sand (RS) and recycled ceramic tiles (RCT) were used as fine aggregates. The coarse aggregate (CA) in the mix was granite chippings. Portland Limestone cement was used with a 32.5R strength class, conforming to NIS 444-1 standard [42]. It was manufactured by United Cement Company of Nigeria. River sand was obtained from a mining site at Ikot Ekong, Akwa Ibom State, while granite chippings were from a quarry in Akamkpa, Cross River State, also in Nigeria. RCT consisted of recycled floor and wall tiles. These were tiles, as shown in Figure 2(a), which were either cracked or broken during transportation and distribution. They were obtained from a dealer in Uyo. The tiles were broken into smaller pieces and crushed into the required size using a hammer mill (Figure 2(b)) to obtain a fine aggregate. Preliminary tests were done on the aggregates and cement following British standards. These tests included determination of their particle size distributions, specific gravity, and bulk density as well as an X-ray fluorescence test.

(a) (b)

Figure 2 Recycled ceramic tiles before (a) and after (b) crushing

2.2 Methods

The methodology used in this study involved preparation and characterization of materials, design of experiments, production of test samples, testing of samples and finally formulation and testing of Scheffe's regression models.

2.2.1 Design of experiments

Five design components were used. The data was fitted to Scheffe's second-degree polynomial. The mixture experiment was therefore an augmented {5, 2} simplex centroid design developed with the aid of a commercial statistical software package, Minitab 16. The design simplex is shown in Figure 3, while the design matrix for the augmented {5, 2} simplex is presented in Table 1. The points in the simplex were numbered according to their run order employing randomization and replication. There were 21 design points with 27 runs. The 15 design points based on Equation 7 were augmented with additional six design points that included the centroid of the simplex and midpoints between each vertex and the centroid. The additional points were all within the simplex and served as check points. The experiments were replicated at the five vertices and the centroid. From the design matrix and simplex, the five replicated runs that represent the five mixes at the vertices of the simplex were: Run Orders 10 and 22 (Vertex X_1), 3 and 4 (Vertex X_2), 11 and 18 (Vertex X_3), 6 and 12 (Vertex X_4), then 8 and 13 (Vertex X_5). The results at these vertices defined the boundary of the simplex and the resulting models. From Equations 5 and 6, summation of the components for each run equals unity. The lower and upper boundaries for each component were 0 and 1, respectively.

2.2.2 Pseudo- and actual components

The points in Scheffe's simplex lattice design are usually expressed in terms of pseudo-components. To transform the pseudo-components to actual concrete mix ratios, the relationship expressed as Equation 10 was used, where *X* is a column matrix of pseudo-components at each run, while *Z* is a column matrix of real component mix ratios. *A* is a square matrix of actual concrete mix ratios (real components) that correspond to the pure blends at the five vertices of the simplex. These mixes were selected by the researchers based upon our experience and a series of trial mixes.

$$Z = AX \tag{10}$$

The selected ratios of water (Z_1), cement (Z_2), sand (Z_3), RCT (Z_4) and CA (Z_5), representing the pure blends at the respective vertices of the simplex were as follows:

X_1 [0.6 : 1 : 0 : 1.5 : 3],
X_2 [0.5 : 1 : 1.5 : 0 ; 3],
X_3 [0.65 : 1 : 2.5 : 0 : 4.5],
X_4 [0.4 : 1 : 1 : 0 : 2] and
X_5 [0.45 : 1 : 0 : 1 : 2]

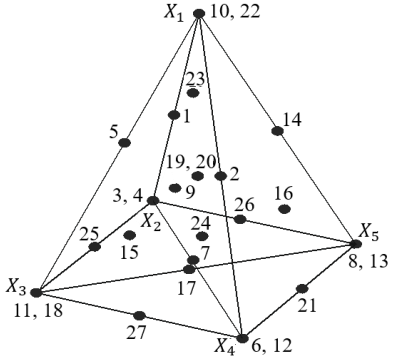

Figure 3 Augmented {5, 2} Scheffe's simplex centroid lattice showing design points and run orders

Table 1 Design matrix showing pseudo and real components

Run order	Pseudo components					Components in real ratios					% Replacement of sand with RCT
	X_1	X_2	X_3	X_4	X_5	Z_1 Water	Z_2 Cement	Z_3 Sand	Z_4 RCT	Z_5 CA	
1	0.5	0.5	0	0	0	0.55	1	0.75	0.75	3	50.0
2	0.5	0	0	0.5	0	0.5	1	0.5	0.75	2.5	60.0
3	0	1	0	0	0	0.5	1	1.5	0	3	0.0
4	0	1	0	0	0	0.5	1	1.5	0	3	0.0
5	0.5	0	0.5	0	0	0.625	1	1.25	0.75	3.75	37.5
6	0	0	0	1	0	0.4	1	1	0	2	0.0
7	0	0.5	0	0.5	0	0.45	1	1.25	0	2.5	0.0
8	0	0	0	0	1	0.45	1	0	1	2	100.0
9	0.1	0.6	0.1	0.1	0.1	0.51	1	1.25	0.25	2.95	16.7
10	1	0	0	0	0	0.6	1	0	1.5	3	100.0
11	0	0	1	0	0	0.65	1	2.5	0	5	0.0
12	0	0	0	1	0	0.4	1	1	0	2	0.0
13	0	0	0	0	1	0.45	1	0	1	2	100.0
14	0.5	0	0	0	0.5	0.525	1	0	1.25	2.5	100.0
15	0.1	0.1	0.6	0.1	0.1	0.585	1	1.75	0.25	3.7	12.5
16	0.1	0.1	0.1	0.1	0.6	0.485	1	0.5	0.75	2.45	60.0
17	0	0	0.5	0	0.5	0.55	1	1.25	0.5	3.25	28.6
18	0	0	1	0	0	0.65	1	2.5	0	4.5	0.0
19	0.2	0.2	0.2	0.2	0.2	0.52	1	1	0.5	2.9	33.3
20	0.2	0.2	0.2	0.2	0.2	0.52	1	1	0.5	2.9	33.3
21	0	0	0	0.5	0.5	0.415	1	0.5	0.5	2	50.0
22	1	0	0	0	0	0.6	1	0	1.5	3	100.0
23	0.6	0.1	0.1	0.1	0.1	0.56	1	0.5	1	2.95	66.7
24	0.1	0.1	0.1	0.6	0.1	0.46	1	1	0.25	2.45	20.0
25	0	0.5	0.5	0	0	0.575	1	2	0	3.75	0.0
26	0	0.5	0	0	0.5	0.475	1	0.75	0.5	2.5	40.0
27	0	0	0.5	0.5	0	0.525	1	1.75	0	3.25	0.0

Putting these into matrix form, matrix A is:

$$A = \begin{pmatrix} 0.6 & 0.5 & 0.65 & 0.4 & 0.45 \\ 1 & 1 & 1 & 1 & 1 \\ 0 & 1.5 & 2.5 & 1 & 0 \\ 1.5 & 0 & 0 & 0 & 1 \\ 3 & 3 & 4.5 & 2 & 2 \end{pmatrix}$$ and substituting into Equation 10, yields,

$$\begin{pmatrix} Z_1 \\ Z_2 \\ Z_3 \\ Z_4 \\ Z_5 \end{pmatrix} = \begin{pmatrix} 0.6 & 0.5 & 0.65 & 0.4 & 0.45 \\ 1 & 1 & 1 & 1 & 1 \\ 0 & 1.5 & 2.5 & 1 & 0 \\ 1.5 & 0 & 0 & 0 & 1 \\ 3 & 3 & 4.5 & 2 & 2 \end{pmatrix} \begin{pmatrix} X_1 \\ X_2 \\ X_3 \\ X_4 \\ X_5 \end{pmatrix} \quad (11)$$

Equation 11 was used to compute components in real ratios. It was employed for sample preparation in laboratory experiments. Results of the computations are presented in Table 1 with corresponding pseudo-components.

2.2.3 Preparation of test samples

Batching of concrete components was by weight using the real component ratios in Table 1. A total of 27 mixes were done, corresponding to the 27 runs of the design matrix. Mixing, compaction and curing of concrete samples were in accordance with BS EN 12390-2 [43]. For each fresh mix, a slump test was done in duplicate, in accordance with BS EN 12350-2 [44]. Concrete prisms with dimensions of 500 *mm* x 100 *mm* x 100 *mm* and cylinders with a 150 *mm* diameter and 300 mm height (Figure 4) were produced for each mix. Three replicates were produced for each mix. Samples were demolded after about 24 hours and cured by immersion in water for 28 days.

Figure 4 Concrete beam and cylinder samples

2.2.4 Tensile strength test

Tensile strength was determined using a split cylinder test set-up and the procedures described in BS EN 12390-6 [45]. For each test, the respective cylindrical sample was placed on its horizontal axis between the platens of a compression testing machine, as shown in Figure 5. Progressive compressive loads were applied along the horizontal axis of the specimens until failure occurred by splitting along the Centre line. Split tensile strength was computed using Equation 12, where *fst* is the split tensile strength in N/mm^2, *F* is the load at failure in *N*, *L* is length of the specimen in mm and *D* is diameter of specimen in mm. Three samples were tested for each of the 27 runs.

$$f_{st} = \frac{2F}{\pi LD} \tag{12}$$

Figure 5 Loading of sample for split tensile strength test

2.2.5 Flexural strength test

A centre-point loading bending test set-up (Figure 6) and procedures described in BS EN 12390-5 [46] were used to determine flexural strength based on Equation 13, where f_{cf} is the flexural strength in N/mm^2, *L* is the distance between the supporting (lower) rollers, in mm, *b* and d are the width and depth of sample respectively. Three samples were tested for each run.

$$f_{cf} = \frac{FL}{bd^2} \tag{13}$$

Figure 6 Loading of sample for flexural strength test

3. Results

3.1 Material characterizations

Particle size distribution curves of aggregates used in laboratory experiments are presented in Figures 7 and 8, while selected physical properties of aggregates are presented in Table 2. The chemical composition of cement and RCT are shown in Table 3. From Figure 7, both sand and RCT satisfy the overall grading requirement of BS 882:1992 [20] and are therefore suitable for concrete production. Additionally, RCT falls within the coarse grading limits while sand falls within medium grading limits. From Figure 8, CA satisfies the grading requirements for coarse aggregate with nominal size 20 to 5 mm according to BS 882:1992 [20] and as such is also suitable for concrete production. Values of the uniformity coefficient (C_u) and gradation coefficient (C_c) in Table 2 show that RCT has a wider range of particle sizes than sand and CA. It can be classified, as well graded, because its C_u value is greater than 6, while its C_c is between 1 and 3. Specific gravity and bulk density values of RCT were observed to be slightly lower than those of sand, indicating that RCT is a lighter fine aggregate compared to sand. However, these values are within the range found in the literature [11, 20, 47, 48].

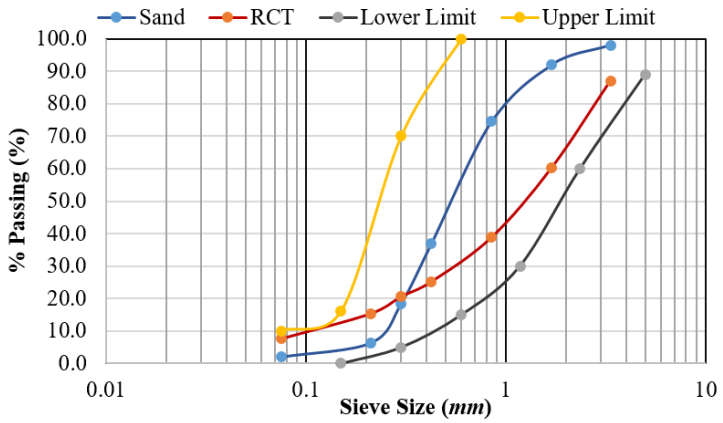

Figure 7 Particle size distribution curve for fine aggregates

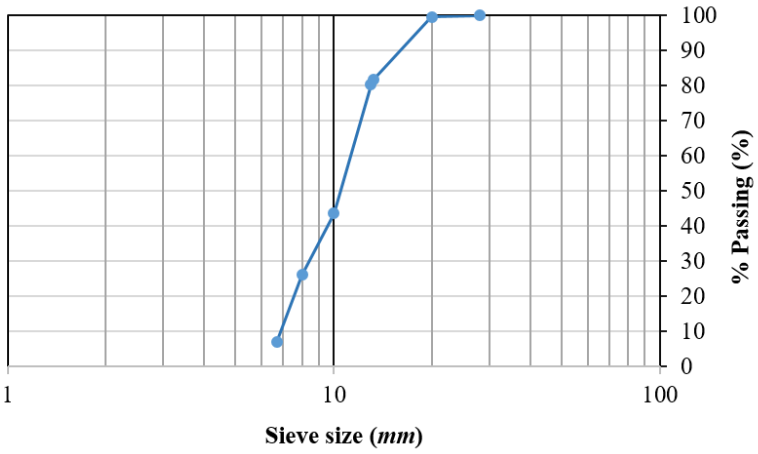

Figure 8 Particle size distribution curve for CA

Table 2 Physical properties of aggregates

Property	Sand	RCT	CA
Specific gravity	2.61	2.40	2.39
Bulk density (kg/m^3)	1635	1373	1386
Uniformity coefficient (C_u)	2.85	17	1.84
Gradation coefficient (C_c)	0.73	1.78	0.87

Table 3 Chemical composition of cement and RCT

Compound	% composition by mass	
	Cement	RCT
Iron oxide (Fe_2O_3)	2.25	3.07
Aluminum oxide (Al_2O_3)	4.73	17.50
Silicon dioxide (SiO_2)	19.84	66.13
Calcium oxide (CaO)	70.32	5.70
Manganese oxide (MnO)	0.01	0.58
Magnesium oxide (MgO)	1.47	2.14
Zinc oxide (ZnO)		0.42
Sulfur trioxide (SO_3)	0.03	-
Sodium oxide (Na_2O)	0.08	0.09
Potassium oxide (K_2O)	0.72	1.02
LOI (Loss of Ignition)	1.01	3.30

3.2 Experimental responses

3.2.1 Workability

For this study, the workability of each mix was measured in terms of slump height. Averaged results are presented in Table 4. Minimum and maximum slump values were 5 mm and 82.5 mm, respectively, representing very low to very high slump values [20]. Slump results show that mixes with high RCT contents are characterized by reduced workability compared to similar mixes with little

or no RCT content. This can be seen by comparing the mix in Run Order 4 with that in Run Order 10. The two mix compositions are similar in terms of cement, fine aggregate and coarse aggregate content except that the latter uses 100% RCT as a fine aggregate, while the former uses 100% sand. However, although mix 4 has a water-cement ratio of 0.5, while the water cement ratio of mix 10 is 0.6, the latter has a far more reduced slump (5.0 mm) than the former (60 mm).

3.2.2 Split tensile strength

Experimental responses for characteristic split tensile strengths of RCT concrete samples in the 27 runs are presented in Table 4, with values ranging from 1.893 to 3.527 N/mm^2. These values define the boundary of the simplex for prediction of characteristic split tensile strengths. The results show that replacing river sand with RCT produces higher tensile strength. This could be seen by comparing results at Vertex X_4 (Run Orders 6 and 12) with those at Vertex X_5 (Run Orders 8 and 13). At the same mix ratio of 1:1:2 (cement: fine aggregate: coarse aggregate), although the latter has a higher water/cement ratio than the former, its tensile strength was higher than that of the former since RCT was used as 100% fine aggregate in the latter mix.

Table 4 Experimental and model responses for characteristics split tensile strengths ($f_{st,\,28}$) and flexural strengths ($f_{cf,\,28}$)

Run order	Real component ratios					%Replacement of sand with RCT	Slump (mm)	Split tensile strength (N/mm^2)		Flexural strength (N/mm^2)	
	Z_1 Water	Z_2 Cement	Z_3 Sand	Z_4 RCT	Z_5 CA			Experimental response	Model response	Experimental response	Model response
1	0.55	1	0.75	0.75	3	50.0	40.0	2.668	2.789	3.299	3.297
2	0.5	1	0.5	0.75	2.5	60.0	45.0	2.624	2.873	4.146	4.041
3	0.5	1	1.5	0	3	0.0	60.0	2.546	2.518	3.420	3.227
4	0.5	1	1.5	0	3	0.0	60.0	2.448	2.518	3.072	3.227
5	0.625	1	1.25	0.75	3.75	37.5	47.5	2.137	2.234	3.353	3.206
6	0.4	1	1	0	2	0.0	75.0	2.583	2.687	3.712	3.791
7	0.45	1	1.25	0	2.5	0.0	47.5	2.681	2.603	3.234	3.158
8	0.45	1	0	1	2	100.0	17.5	3.527	3.423	4.128	4.294
9	0.51	1	1.25	0.25	2.95	16.7	47.5	2.693	2.633	3.206	3.345
10	0.6	1	0	1.5	3	100.0	5.0	3.182	3.059	3.270	3.366
11	0.65	1	2.5	0	4.5	0.0	15.0	1.893	2.070	2.865	3.045
12	0.4	1	1	0	2	0.0	82.5	2.738	2.687	3.834	3.791
13	0.45	1	0	1	2	100.0	10.0	3.375	3.423	4.429	4.294
14	0.525	1	0	1.25	2.5	100.0	10.0	3.484	3.532	4.568	4.447
15	0.585	1	1.75	0.25	3.7	12.5	22.5	2.579	2.343	3.390	3.324
16	0.485	1	0.5	0.75	2.45	60.0	10.0	3.136	3.144	3.921	4.072
17	0.55	1	1.25	0.5	3.25	28.6	15.0	2.589	2.747	3.812	3.670
18	0.65	1	2.5	0	4.5	0.0	20.0	2.166	2.070	3.048	3.045
19	0.52	1	1	0.5	2.9	33.3	25.0	2.837	2.745	3.709	3.661
20	0.52	1	1	0.5	2.9	33.3	35.0	2.869	2.745	3.556	3.661
21	0.425	1	0.5	0.5	2	50.0	5.0	3.055	3.055	4.244	4.043
22	0.6	1	0	1.5	3	100.0	5.0	3.113	3.059	3.489	3.366
23	0.56	1	0.5	1	2.95	66.7	15.0	2.900	2.895	3.413	3.700
24	0.46	1	1	0.25	2.45	20.0	52.5	2.775	2.718	3.642	3.719
25	0.575	1	2	0	3.75	0.0	10.0	2.254	2.294	3.372	3.136
26	0.475	1	0.75	0.5	2.5	40.0	40.0	2.918	2.971	3.651	3.761
27	0.525	1	1.75	0	3.25	0.0	70.0	2.444	2.379	3.323	3.418

3.2.3 Flexural strength

Table 4 also presents experimental responses for characteristic flexural strengths for the 27 runs with values ranging from 2.865 to 4.568 N/mm^2. These values define the boundary of the proposed flexural strength model. The trend of flexural strength values with respect to replacement of sand with RCT is similar to that of split tensile strength.

3.3 Scheffe's regression equations

Model calibration was done using the respective experimental responses in Table 4 with the aid of Minitab 16. The models are expressed in terms of pseudo-components.

3.3.1 Scheffe's equation for split tensile strength

Scheffe's regression polynomial for tensile strength was fitted to the split tensile strength data in Table 4 based on Equation 4. To avoid overfitting the model, backward elimination procedure of stepwise regression was used to eliminate insignificant model terms. Thus, the resulting number of terms was less than 15, as it is based on Equations 4 and 7. Table 5 shows estimated model coefficients for tensile strength with the associated statistics at a 95% confidence level, while Table 6 presents the results of analysis of variance (ANOVA). From the ANOVA table, both linear and quadratic sources are significant. Each has a *p*-value less than 0.05. However, it has been a standard practice to select the highest degree model as long as it is significant [4, 49]. Hence, the quadratic model was selected. Therefore, if the five vertices of the designed {5, 2} simplex lattice are represented in pseudo-form as X_1, X_2, X_3, X_4 and X_5 respectively, then tensile strength model based on Equation 4 is given as:

$$\hat{y} = 3.059X_1 + 2.518X_2 + 2.070X_3 + 2.687X_4 + 3.423X_5 - 1.324X_1X_3 + 1.162X_1X_5 \quad (14)$$

Table 5 Estimated regression coefficients for the split tensile strength model

Term	Coeff	SE coeff	T	P
X_1	3.059	0.07699		
X_2	2.518	0.06809		
X_3	2.070	0.07252		
X_4	2.687	0.06809		
X_5	3.423	0.07252		
$X_1 X_3$	-1.324	0.52378	-2.53	0.020
$X_1 X_5$	1.162	0.52378	2.22	0.036
S = 0.123513, r^2 = 92.74%, r^2 *(pred)* = 70.47%, r^2 *(adj)* = 70.47%				

Legend: Coeff = Coefficients of Terms; SE Coeff = Standard Error; T = t-test value; P = p-value; S = Variance;

Table 6 Analysis of variance for the split tensile strength model

Source	DF	Seq SS	Adj SS	Adj MS	F	P
Regression	6	3.89900	3.89900	0.64983	42.60	0.000
Linear	4	3.72053	2.82617	0.70654	46.31	0.000
Quadratic	2	0.17847	0.17847	0.08923	5.85	0.010
X_1X_3	1	0.10338	0.09755	0.09755	6.39	0.020
X_1X_5	1	0.07509	0.07509	0.07509	4.92	0.038
Residual error	20	0.30511	0.30511	0.01526		
Lack-of-fit	14	0.23658	0.23658	0.01690	1.48	0.328
Pure error	6	0.06852	0.06852	0.01142		
Total	26	4.20411				

Legend: DF = Degrees of Freedom; Seq SS = Sequential Sum of Squares; F = F-value; Adj SS = Adjusted Sum of Squares; Adj MS = Adjusted Mean Squares;

3.3.2 Scheffe's equation for flexural strength

Using the experimental responses for flexural strength in Table 4, Scheffe's augmented simplex lattice regression equation was fitted based on Equation 4. Again, backward elimination procedure of stepwise regression was used. The resulting model estimated coefficients and other statistical information at a 95% confidence level, are as presented in Table 7. ANOVA results are presented in Table 8. From these results, both the linear and quadratic forms are significant since each has a p-value less than 0.05. Hence, the quadratic model was selected and the resulting model for flexural strength is given as:

$$\hat{y} = 3.366X_1 + 3.227X_2 + 3.045X_3 + 3.791X_4 + 4.294X_5 + 1.848X_1X_4 + 2.469X_1X_5 - 1.403X_2X_4 \quad (15)$$

Table 7 Estimated regression coefficients for the flexural strength model

Term	Coeff	SE coeff	T	P
X_1	3.366	0.10224		
X_2	3.227	0.09635		
X_3	3.045	0.09041		
X_4	3.791	0.10224		
X_5	4.294	0.09635		
$X_1 X_4$	1.848	0.69577	2.66	0.016
$X_1 X_5$	2.469	0.69652	3.54	0.002
$X_2 X_4$	-1.403	0.69652	-2.01	0.058
S = 0.163990, r^2 = 89.30%, r^2 *(pred)* = 37.94%, r^2 *(adj)* = 85.36%				

Table 8 Analysis of variance for the flexural strength model

Source	DF	Seq SS	Adj SS	Adj MS	F	P
Regression	7	4.2640	4.2640	0.60914	22.65	0.000
Linear	4	3.6542	2.8968	0.72420	26.93	0.000
Quadratic	3	0.6098	0.6098	0.20328	7.56	0.002
X1X4	1	0.1829	0.1896	0.18962	7.05	0.016
X1X5	1	0.3178	0.3379	0.33795	12.57	0.002
X2X4	1	0.1092	0.1092	0.10916	4.06	0.058
Residual Error	19	0.5110	0.5110	0.02689		
Lack-of-Fit	13	0.3452	0.3452	0.02656	0.96	0.556
Pure Error	6	0.1657	0.1657	0.02762		
Total	26	4.7750				

3.4 Test of adequacy and model validation

Adequacy and validation of the models were determined using normal probability plots and ANOVA tables employing lack-of-fit testing at a 95% confidence level. Other validation criteria were based on r^2, predicted r^2 and adjusted r^2 values.

3.4.1 Tensile strength model

A normal probability plot of tensile strength model residuals is presented in Figure 9. The plot shows a close distribution of the model residuals along a reference line with a *p*-value of 0.640 (which is greater than 0.05). The null hypothesis was that the data (model residuals) follow a normal distribution curve and this hypothesis could not be rejected because the plot's *p*-value was greater than 0.05. Hence, the model residuals follow a normal distribution curve and this justifies the use of ANOVA. From the ANOVA results in Table 6, the model's *lack-of-fit* has a *p*-value of 0.328. This value is greater than 0.05. Thus, the model does not show a significant *lack-of-fit*. From Table 5, the model has an r^2 value of 92.74%, adjusted r^2 of 90.57% and predicted r^2 of 70.47%. These high values reflect the quality of the model. This, in addition to the earlier mentioned points, confirms the adequacy of Equation 14 in predicting characteristic tensile strengths of RCT concrete.

3.4.2 Flexural strength model

Again, the normal probability plot in Figure 10 shows a close distribution of model residuals along a reference line. The plot has a *p*-value of 0.154 (which is greater than 0.05). Hence, the null hypothesis cannot be rejected, meaning that the residuals of the model follow a normal distribution and this justifies the use of ANOVA. The analysis of variance tables in Table 8 shows an insignificant *lack-of-fit* with a *p*-value of 0.556. These and other statistical values in Table 7, an r^2 value of 89.30%, adjusted r^2 of 85.36% and predicted r^2 of 37.94%, confirm the adequacy of Equation 15.

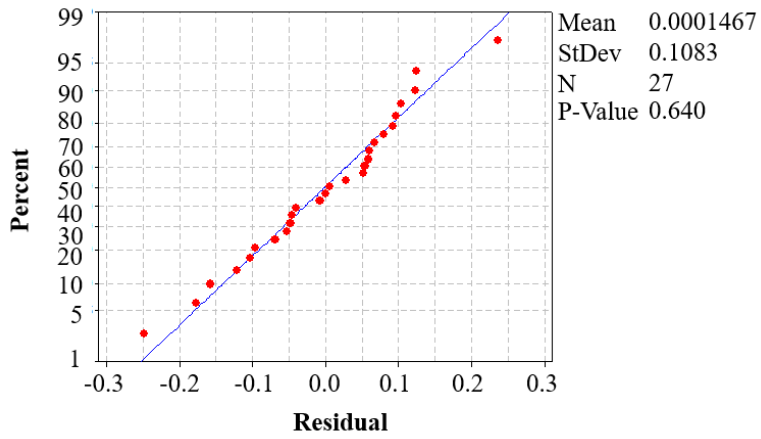

Figure 9 Normal probability plot for the split tensile strength model residuals

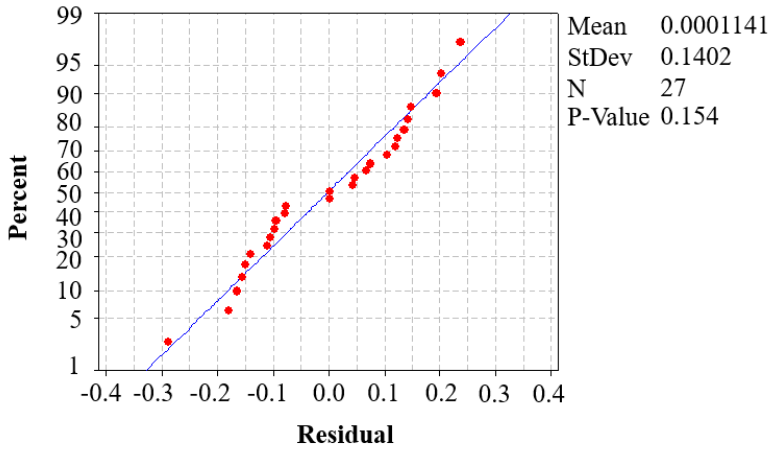

Figure 10 Normal probability plot for the flexural strength model residuals

4. Discussion

The results of preliminary tests on materials used in this study show that RCT is a suitable material that can be used as fine aggregate in concrete production. It covers a wide range of particle sizes, is well graded and satisfies the gradation requirements of BS 882:1992. However, incorporation of this material as fine aggregate has been found to reduce workability of fresh concrete. This has been previously reported [13, 47, 50] and obviously results from its physical properties. Ceramic waste aggregates are usually porous and rough textured with high water absorption properties [13]. A combination of these properties along with its usual and irregularly shaped particles reduces workability of such fresh concrete mixes.

Using Scheffe's simplex theory, polynomial model equations were formulated for predicting tensile and flexural strengths of concrete incorporating RCT as fine aggregates. Stepwise regression was used during model formulation. Insignificant variables were removed from the model terms to avoid overfitting. This practice improved the resulting model. Its benefits are demonstrated in the model statistics shown in Tables 5-8 and Figures 6 and 7. Both model equations show insignificant lack-of-fit, as presented in Tables 6 and 8. The high r^2, adjusted r^2 and predicted r^2 values in Tables 6 and 8 show the better quality of the models. While r^2 and adjusted r^2 values show how well the models fit their respective data, the high predictive r^2 values indicate how well the formulated models can predict new responses outside the design points. This validates the models.

From the formulated models, the maximum predicted tensile strength was 3.560 N/mm^2, occurring between vertices X_1 and X_5 of the simplex and corresponding to a mix ratio of 0.5015:1:0:1.1717:2.3434 for water, cement, sand, RCT and CA, respectively. The maximal response for flexural strength was 4.534 N/mm^2, which also existed between vertices X_1 and X_5 of the simplex and corresponding to a mix ratio of 0.4968:1:0:1.156:2.312. The two mix ratios show that maximum strength values were obtained from mixes with 100% RCT as fine aggregate and indicates that replacing sand with RCT improves concrete strength properties. The minimum predictable tensile strength was 2.049 N/mm^2, between vertices X_1 and X_3 of the simplex with a mix ratio of 0.6437:1:2.1837:0.1898:4.3102. The minimum response for flexural strength was 3.045 N/mm^2 existing at Vertex X_3.

5. Conclusions

This study successfully developed mathematical models for predicting and optimizing the tensile and flexural strength of concrete incorporating RCT as fine aggregates. This was achieved using augmented Scheffe's simplex lattice theory. Results of preliminary tests show that RCT is suitable for use as a fine aggregate in concrete production. Responses predicted by the formulated models are in good agreement with experimentally observed data. The models were tested using analysis of variance and normal probability plots of model residuals. They were found adequate and hence are valid. The quality of the models is also reflected in their high r^2, adjusted r^2 and predicted r^2 values. Maximum and minimum predictable tensile strengths were 3.560 N/mm^2 and 2.049 N/mm^2, while the corresponding values for flexural strength were 4.534 N/mm^2 and 3.045 N/mm^2. It is established that addition of RCT can improve the tensile and flexural strength of concrete.

6. Acknowledgement

The authors acknowledge the financial support of the Tertiary Education Trust Fund (TETFund) Nigeria for the PhD studies of Edidiong E. Ambrose.

7. References

[1] Tahar Z, Benabed B, Kadri E, Ngo T, Bouvet A. Rheology and strength of concrete made with recycled concrete aggregate as replacement of natural aggregates. Epitoanyag JSBCM. 2020;72(2):48-58.
[2] Ambrose EE, Forth JP. Influence of relative humidity on tensile and compressive creep of concrete amended with ground granulated blast-furnace slag. Niger J Tech. 2018;37(1):19-27.
[3] Ikponmwosa EE, Ehikhuenmen SO. The effect of ceramic waste as coarse aggregate on strength properties of concrete. Niger J Tech. 2017;36(3):691-6.
[4] Anya UC. Models for predicting the structural characteristics of sand-quarry dust blocks. Nsukka: University of Nigeria; 2015.
[5] Wongkvanklom A, Sata V, Sanjayan JG, Chindaprasirt P. Setting time, compressive strength and sulfuric acid resistance of a high calcium fly ash geopolymer borax. Eng Appl Sci Res. 2018;45(2):89-94.
[6] Hadavand B, Imaninasab R. Assessing the influence of construction and demolition waste materials on workability and mechanical properties of concrete using statistical analysis. Innovat Infrastuct Solut. 2019;4:1-11.
[7] Ambrose EE, Ekpo DU, Umoren IM, Ekwere US. Compressive strength and workability of laterized quarry sand concrete. Niger J Tech. 2018;37(3):605-10.
[8] Kannan MK, Aboubakr SH, El-Dieb AS, Taha MM. High performance concrete incorporating ceramic wastes powder as large partial replacement of Portland cement. Constr Build Mater. 2017;144:35-41.
[9] Zimbili O, Salim W, Ndambuki M. A review on the usage of ceramic wastes in concrete production. Int J Civ Environ Struct Const Archit Eng. 2014;8(1):91-5.
[10] Gonzalez-Coromina A, Etxeberria M. Properties of high-performance concrete made with recycled fine ceramic and coarse mixed aggregate. Constr Build Mater. 2014;68:618-26.
[11] Higashiyama H, Yagishita F, Sano M, Takahashi O. Compressive strength and resistance to chloride penetration or mortars using ceramic as fine aggregate. Constr Build Mater. 2012;26:96-101.
[12] Shruthi HG, Gowtham ME, Samreen T, Syed RP. Re-use of ceramic waste as aggregate in concrete. Int Res J Eng Tech. 2016;3(7):115-9.
[13] Halicka A, Ogrodnik P, Zegardlo B. Using ceramic sanitary ware waste as concrete aggregate. Const Build Mater. 2013;48: 295-305.
[14] Awoyera PO, Ndambuki JM, Akinmusuru JO, Omole OD. Characterization of ceramic waste aggregate. HBRC J. 2018;14(3):282-7.
[15] Elci H. Utilisation of crushed floor and wall tile wastes as aggregate in concrete production. J Cleaner Prod. 2016;112:742-52.

[16] Rashid K, Razzaq A, Ahmad M, Rashid T, Tariq S. Experimental and analytical selection of sustainable recycled concrete with ceramic waste aggregate. Const Build Mater. 2017;154:829-40.
[17] Nepomuceno MC, Isidoro RA. Mechanical performance evaluation of concrete made with recycled ceramic coarse aggregate from industrial brick waste. Const Build Mater. 2018;165:284-94.
[18] Bartosz Z, Maciej S, Pawel O. Ultra-high strength concrete made with recycled aggregate from sanitary ceramic wastes-the method of production and the interfacial transition zone. Const Build Mater. 2016;122:736-42.
[19] Paewchompoo N, Yodsudjai W, Suwanvitaya P, Iwanami M. Corrosion-induced cracking in recycled aggregate concrete (RAC). Eng Appl Sc Res. 2020;47(2):145-52.
[20] Neville AM. Properties of concrete. 5th ed. London: Pearson Education; 2011.
[21] Marke MO, Marke AI. Comparative evaluation of the flexural strength of concrete and colcrete. Niger J Tech. 2010;29(1): 13-22.
[22] Iqbal KM. Analytical model for the strength prediction of HPC consisting of cementitious composites. Archit Civ Eng Environ. 2009;1:89-96.
[23] Chidiac SE, Moutassem F, Mahmoodzadeh F. Compressive strength model for concrete. Mag Concr Res. 2013;65(9):557-72.
[24] Popovics S, Ujhelyi J. Contribution to the concrete strength versus water-cement ratio relationship. J Mater Civ Eng. 2008;20(7):459-63.
[25] Oztas A, Pala M, Ozbay E, Kanca E, Caglar N, Bhatti MA. Predicting the compressive strength and slump of high strength concrete using neural network. Constr Build Mater. 2006;20(9):769-75.
[26] Shariati M, Mafipour MS, Mehrabi P, Karzan MA. Prediction of concrete strength in presence of furnace slag and fly ash hybrid ANN-GA (Artificial Neural Network-Genetic Algorithm). Smart Struct Syst. 2020;25(2):183-195.
[27] Khashman A, Akpinar P. Non-destructive prediction of concrete compressive strength using neural networks. Procedia Comput Sci. 2017;108:2358-62.
[28] Chen L. A multiple linear regression prediction of concrete compressive strength based on physical properties of electric arc furnace oxidizing slag. Int J Appl Sci Eng. 2010;2(7):153-8.
[29] Hariharan AR, Santhi AS, Mohan Ganesh G. Statistical model to predict the mechanical properties of binary and ternary blended concrete using regression analysis. Int J Civ Eng. 2015;13(3):331-40.
[30] Chopra P, Sharma RK, Kumar M. Regression models for the prediction of compressive strength of concrete with & without fly ash. Int J Latest Trends Eng Tech. 2014;3(4):400-6.
[31] Tepecik A, Altin Z, Erturan S. Modeling compressive strength of standard CEM-I 42.5 cement produced in Turkey with stepwise regression method. J Chem Soc Pak. 2009;31(2):214-20.
[32] Allahverdi A, Mahinroosta M, Pilehvar S. A temperature-age model for prediction of compressive strength of chemically activated high phosphorous slag content cement. Int J Civ Eng. 2017;15:839-47.
[33] Allahverdi A, Mahinroosta M. A model for prediction of compressive strength of chemically activated high phosphorous slag content cement. Int J Civ Eng. 2014;12(4):481-7.
[34] Onuamah PN, Osadebe NN. Development of optimized strength model of lateritic hollow block with 4% mound soil inclusion. Niger J Tech. 2015;34(1):1-11.
[35] Mama BO, Osadebe NN. Comparative analysis of two mathematical models for prediction of compressive strength of sancrete blocks using alluvial deposit. Niger J Tech. 2011;30(3):82-9.
[36] Okafor FO, Oguaghamba O. Procedures for optimization using Scheffe's model. J Eng Sci Appl. 2010;7(1):36-46.
[37] Attah IC, Etim RK, George UA, Bassey OB. Optimization of mechanical properties of rice husk ash concrete using Scheffe's theory. SN Appl Sci. 2020;2:928.
[38] Scheffe H. Experiment with mixtures. J R Stat Soc. 1958;20(2):344-60.
[39] Akhnazarova S, Kafarov V. Experiment optimization in chemistry and chemical engineering. Moscow: MIR Publishers; 1982.
[40] Osadebe NN, Mbajiorgu CC, Nwakonobi TU. An optimization model development for laterized concrete mix proportioning in building constructions. Niger J Tech. 2007;26(1):37-45.
[41] Onyelowe K, Alaneme G, Igboayaka C, Orji F, Ugwuanyi H, Van DB, et al. Scheffe optimization of swelling, California bearing ratio, compressive strength, and durability potentials of quarry dust stabilized soft clay soil. Mater Sci Energy Tech. 2019;2: 67-77.
[42] NIS 444-1. Composition, specification and conformity criteria for common cements. Abuja: Standard Organization of Nigeria; 2008.
[43] BS EN 12390-2. Testing hardened concrete-Part 2: Making and curing specimens for strength tests. London: British Standard Institute; 2009.
[44] BS EN 12350-2. Testing fresh concrete-part 2: Slump test. London: British Standard Institute; 2009.
[45] BS EN 12390-6. Testing hardened concrete-part 6: Tensile splitting strength of test specimens. London: British Standard Institute; 2009.
[46] BS EN 12390-5. Testing hardened concrete-part 5: Flexural strength of test specimens. London: British Standard Institute; 2009.
[47] Awoyera PO, Akinmusuru JO, Ndambuki JM. Green concrete production with ceramic wastes and laterite. Const Build Mater. 2016;117:29-36.
[48] Binici H. Effect of crushed ceramic and basalt pumics as fine aggregates on concrete mortar properties. Const Build Mater. 2007;21:1191-7.
[49] Simon MJ. Concrete mixture optimization using statistical methods: final report. Virginia, USA: Federal highway administration, Infrastructure Research and Development; 2003.
[50] Torkittikul A, Chaipanich A. Utilization of ceramic waste as fine aggregate within Portland cement and fly ash concrete. Cem Conc Compos. 2010;32:440-9.